water

MDPI

Article

Spatio-Temporal Dynamics of Riverine Nitrogen and Phosphorus at Different Catchment Scales in Huixian Karst Wetland, Southwest China

Linyan Pan [1], Junfeng Dai [2,3,*], Zhiqiang Wu [2,3,*], Zupeng Wan [1], Zhenyu Zhang [1], Junlei Han [1], Zhangnan Li [1], Xiaolin Xie [1] and Baoli Xu [1]

1 College of Environmental Science and Engineering, Guilin University of Technology, Guilin 541004, China; ann-fred@163.com (L.P.); wzp7332731@163.com (Z.W.); zhangzy298@163.com (Z.Z.); han1057396887@163.com (J.H.); 17832400228@163.com (Z.L.); xl059526@163.com (X.X.); blxu@glut.edu.cn (B.X.)

2 Guangxi Key Laboratory of Environmental Pollution Control Theory and Technology, Guilin University of Technology, Guilin 541004, China

3 Collaborative Innovation Center for Water Pollution Control and Water Security in Karst Region, Guilin University of Technology, Guilin 541004, China

* Correspondence: whudjf@163.com (J.D.); wuzhiqiang@glut.edu.cn (Z.W.); Tel.: +86-13977396045 (J.D.); +86-773-2537332 (Z.W.)

Received: 7 August 2020; Accepted: 15 October 2020; Published: 19 October 2020

check for updates

Abstract: Spatio-temporal dynamics of riverine nitrogen (N) and phosphorus (P) in karst regions are closely linked to hydrological conditions, human activities and karst features in upstream catchments. From October 2017 to September 2019, we undertook 22 sampling campaigns in 11 nested catchments ranging from 21.00 to 373.37 km^2 in Huixian karst wetland to quantify forms, concentrations, and fluxes of riverine total nitrogen (TN) and total phosphorus (TP), and to identify spatial and temporal variations of nutrients transfer from upstream to downstream, tributaries (Mudong River and Huixian River) to the main stem (Xiangsi River) in the dry and wet seasons. Considering the hydrological conditions, human activities and karst features within upstream catchments, the following three spatial and temporal variations of riverine nutrients were found over the monitoring period: (1) the dynamics of riverine nitrogen and phosphorus varied seasonally with hydrological conditions; (2) the spatial disparities of riverine nitrogen and phosphorus were induced by different human activities within catchment scales; (3) the dynamics of riverine nitrogen and phosphorus varied similarly at spatial scale restricted by karst features. The findings from this study may improve our understanding of the influence of hydrological conditions, human activities and karst features on nitrogen and phosphorus variations in river waters at different spatial and temporal scales in the Huixian karst wetland basin, and will help managers to protect and restore river water environments in karst basin from a catchment-scale perspective.

Keywords: total nitrogen; total phosphorus; riverine nutrient; hydrogeology; catchment; karst

1. Introduction

The eutrophication of surface waters has become an increasingly significant global water quality concern [1,2]. Direct and indirect effects from human activities, such as the excessive use of fertilizers in agriculture and the indiscriminate discharge of untreated sewage, have dramatically increased the nitrogen (N) and phosphorus (P) loading to aquatic ecosystems [3,4]. River water is suffering from nitrogen and phosphorus pollution in karst areas [5] where water resources are particularly valuable [6,7]. It is estimated that carbonate karst covers approximately 15% of the Earth's ice-free continental areas, and supplied water resources for about one-quarter of the Earth's population [8]. Soils in karst regions are thin, fragmented, fragile and slow to form [9–11], thus the limited farmland area in karst regions is so poor for food production that requires more fertilizer, resulting in greater complexity and vulnerability of ecological environment under the specific hydrogeological conditions.

Characterized by gullies, gaps, skylights and funnels in the surface and conduits, fractures and matrix flow under the surface [12], the karstic aquifer is particularly vulnerable to anthropogenic contamination due to its rapid transport from surface to groundwater, and then to lowland rivers fast through fracture networks within the karst architecture. The rapid flow pathways through the unique karst surface–subsurface binary spatial structure [13] shorten contaminant residence time, which reduces capacity for attenuation, affects surface receiving water quality and poses a serious threat to karst water ecosystems [14,15]. Nutrient loading in surface water has been predicted to increase through the middle of the century for more precipitation in both frequency and magnitude [16]. Therefore, long-term field-based monitoring of nitrogen and phosphorus in karst surface water systems is necessary to obtain series of data on nitrogen and phosphorus dynamics in order to identify the main influences on temporal and spatial dynamic characters of nutrients export [17].

The water cycle is the main driver and carrier for nutrients cycling [18], and plays an important role in nitrogen and phosphorus transfer. N and P flow with river waters along lateral (from upstream to downstream, tributaries to the main stem) and longitudinal (from surface to subsurface, and then recharge to surface lowland rivers), influenced by catchment attributes (e.g., soils, geology, land use, hydrological conditions and human activities) [19–21], accompanied by the transformation of different forms [22,23]. Spatial and temporal variations of nitrogen and phosphorus at the outlet were significantly correlated with the attributes of the catchment which is the basic unit of the terrestrial-aquatic ecological cycle system [24]. Analysis of spatio-temporal variations of nitrogen and phosphorus driven by hydrological conditions at different catchment scales help to improve the understanding of the coupled processes between water and nutrient cycling [25,26]. Thus, identifying the spatio-temporal variations of N and P transfer in karst water systems and revealing their influence factors have become one of the focus of international concern in karst ecology [27–30].

Huixian karst wetland is a typical karst water ecosystem in southwest China, and also the largest natural wetland system known in the low-altitude subtropical karst region of China [31]. Currently, the research on Huixian karst wetlands by government and researchers is at early stage of development, yet we know of no long-term monitoring stations for nitrogen and phosphorus that have established in rivers, only a few studies have focused on the stoichiometry characteristics of N and P in its river network, with low and discontinuous monitoring frequency, and few linkage to karst hydrology [32–34]. Most of these studies have focused on concentration analysis and water quality evaluation, neglecting the role of hydrogeology in controlling nutrient transfer and the importance of catchment as a basic unit of both water and nutrient cycling. Few studies have focused on the spatio-temporal variations of N and P driven by hydrological conditions and karst features at different river orders and catchment scales in Huixian karst wetland basin. However, understanding the temporal and spatial dynamics of N and P from the water-nutrients cycling and catchment perspective is crucial for controlling river water quality. Therefore, in our study, data on discharge, concentrations and forms of TN and TP were collected monthly at multiple scales (11 nested catchments ranging from 21.00 to 373.37 km^2 in scale) of 3 connected rivers (from upstream to downstream, tributaries to the main stem) across the Huixian karst wetland basin from October 2017 to September 2019, to investigate the spatio-temporal variations and to identify the influence factors on nutrients transfer in a karst basin.

Monitoring data throughout the whole hydrological years are important to understand the effects of hydrological conditions on nutrient transfer and can also be used for simulation of nutrient transport [35,36]. Catchment-scale field-based monitoring of riverine nutrient dynamics and hydrologic processes was used to investigate the spatial and temporal variations of nitrogen and phosphorus, and to identify the influences of hydrological conditions, human activities and karst features on it over two years (from October 2017 to September 2019). On the other hand, these surveys will be helpful for the government to establish long-term monitoring of nitrogen and phosphorus in the Huixian karst wetlands in the future. The objectives of this study were as follows: (1) quantify the spatial and seasonal variations of riverine nutrient forms, concentrations and mass flux in Huixian karst wetland basin during the monitoring period; (2) identify the effects of hydrological conditions, human activities and karst features on such variations; (3) provide suggestions for controlling nitrogen and phosphorus pollution of the river system in Huixian Karst Wetland basin to further improve the quality of river waters.

2. Materials and Methods

2.1. Study Area

Huixian karst wetland basin (E 110°04′–110°16′, N 24°55′~25°18′, elevation 59–974 m, 373.37 km^2) is located in the southwest of Guilin City, Guangxi Province, China (Figure 1). The region has a typical subtropical humid monsoon climate with a mean annual precipitation of 1853.7 mm, a mean annual temperature of 20 °C. The landform is characterized by low hills and hilly in the high north and south, karst peak cluster-depression and peak forest plain in the low center. The soil is classified as red-yellow soil, paddy soil, limestone soil and swamp soil [37]. The soil overlying the carbonate rock varies from 0.0 to 40 m in depth.

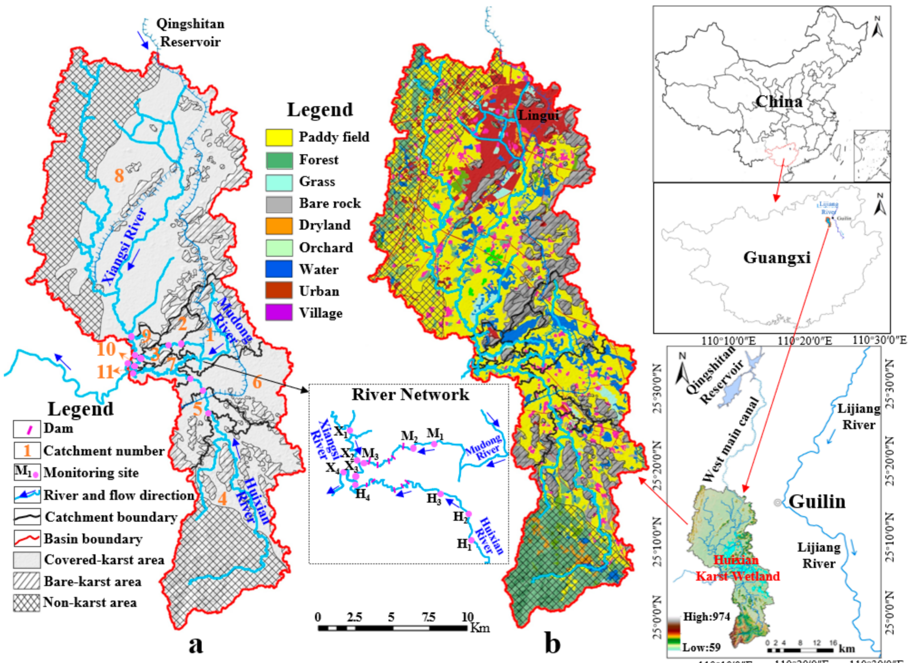

Figure 1. Map of the Huixian karst wetland basin showing (**a**) distribution of the eleven sampling sites (M_1–M_3, H_1–H_4 and X_1–X_4) and the eleven catchments (1–11); and (**b**) the land use types.

The catchment contains one vice-city (Lingui district) and 15 administrative villages that consist of approximately 350,000 permanent urban population, 25,000 inhabitants, several fish farms on scale, and livestock farms on scale or decentralized with several to hundreds of animals. The karst landforms are classified as non-karst, bare karst and covered karst areas. Paddy field, forest and brush are the dominant land-use types in the basin (Table 1). Forests are generally distributed in the non-karst areas, while brushes are on the bare karst areas. Paddy fields are the largest share of land-use and generally distributed in the covered karst areas. Paddy rice is planted twice a year in mid-April and mid-July, and the annual fertilizer application rates for paddy rice are approximately 700 kg N and 225 kg P ha^{-1}year^{-1}, respectively.

Table 1. Distribution of the eleven monitoring sites (M_1–M_3, H_1–H_4 and X_1–X_4), catchments (1–11), and the share of karst and land use area in Huixian karst wetland basin.

Rivers		Monitoring Sites (Index in Figure 2)	Catchments Included	Upstream Area (km^2)	Area (Expressed as Percent of Total Area) (%)											
					Karst			Land Use								
					Non-Karst	Bare Karst	Covered Karst	Paddy Field	Forestland	Grassland	Brush Land	Village	Urban	Dry Land	Orchard	Water
Tributaries	Mudong River	M_1	1	21.00		17.7	82.3	51.3		5.7	17.7	1.3			1.2	22.8
		M_2	1~2	25.64		21.9	78.1	43.4		5.9	21.9	1.1			1.1	26.7
		M_3	1~3	28.00		22.7	77.3	42.6		7.3	22.7	1.0			1.1	25.3
	Huixian River	H_1	4	81.46	59.5	13.9	26.6	13.4	41.1	8.0	13.9	1.4		15.3	4.9	2.0
		H_2	4~5	96.00	50.5	16.2	33.3	17.9	34.9	7.6	16.2	2.1		15.1	4.2	2.0
		H_3	4~6	121.63	39.9	13.9	46.2	24.5	28.4	12.4	13.9	2.9		12.0	3.9	2.0
		H_4	4~7	127.37	38.1	13.5	48.4	27.4	27.1	12.2	13.5	2.8		11.4	3.7	1.9
Main river	Xiangsi River	X_1	8	214.51	36.1	11.3	52.5	33.7	7.4	8.8	11.3	1.5	27.5	7.4	0.8	1.6
		X_2	8~9	217.18	35.7	11.6	52.7	33.8	7.3	8.8	11.6	1.5	27.0	7.5	0.7	1.8
		X_3	1~3, 8~10	245.72	31.5	12.8	55.7	34.9	6.5	8.7	12.8	1.5	23.9	6.6	0.7	4.5
		X_4	1~11	373.37	33.7	13.3	53.0	32.4	13.5	9.9	13.3	1.9	15.7	8.3	1.8	3.6

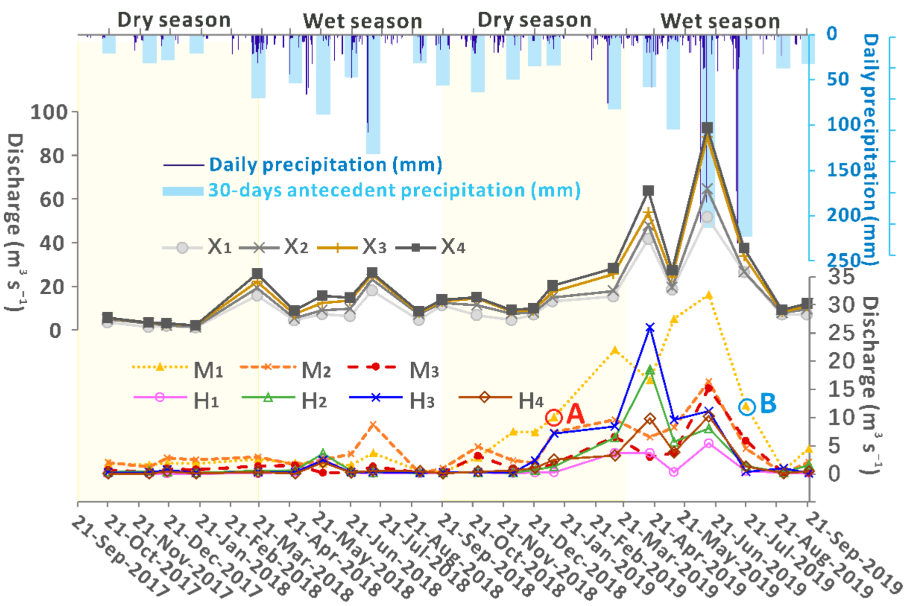

Figure 2. The time series of discharge at the eleven monitoring sections, the daily precipitation and the 30-days antecedent precipitation (referred to the total amount of precipitation over the last 30 days). The light-yellow area represents the dry season. The observation A after rain events in the dry season and observation B during low-flow period in the wet season had similar flow conditions.

The Xiangsi River main stem and tributary Huixian River run down from the non-carbonate highlands in north and south respectively and both flow into the carbonate lowland of the center where they merge with tributary Mudong River which originates from karst springs in the middle east, and then flow into the lower reaches of the Xiangsi River (Figure 1a). The center of the basin is dominated by karst landforms, and the eastern boundary of the basin is the water divided area of the Lijiang (Gui) river and Luoqing (Liu) river. According to the field survey, there are five small dams storing water in the approximately 3 km long channel between the M_2 and M_3 sections of the Mudong River, which are used to pump water to fish ponds and rice fields on the river banks. In addition, there are five small dams in the approximately 8 km long channel between the H_3 and H_4 sections of the Huixian River, which are used to raise the water level of the river so that the water can flow into canals to irrigate farmland (Figure 1).

2.2. Catchments Delineation

Eleven monitoring sections of three rivers were selected as sampling sites for discharge and riverine N and P levels after investigating the spatial distribution of the river network systems in the studied basin. Each river section was defined as the outlet of upstream catchment, and the boundary of each catchment was delineated based on the digital elevation model (DEM) of the studied area in ArcGIS™ 10.2 software (ESRI, Redlands, CA, USA). Then, land use areas in each catchment were determined based on the DEM. Detailed information for the delineated catchments is provided in Table 1 and Figure 1. In addition, daily rainfall data were obtained from the Guilin weather station (about 10 km northeast from the Huixian karst wetland basin) run by the national weather service.

2.3. Data Collection and Analysis

From October 2017 to September 2019, water depth and velocity at the outlet of each catchment scale was monitored monthly, and the water samples were collected for N, P concentration and form analysis. The flow velocity of the river water was measured in field by hand-held Electric Wave Flow Meter (Stalker II SVR, Applied Concept Inc., Brannon, TX, USA), and the cross-section flow area of the river was measured by channel geometry and water depth using a ruler. The cross-section discharge (m^3/s) of each catchment outlet was estimated by combining the measured cross-section flow area (m^2) with the observed flow velocity (m/s).

Two methods were used to collect water samples depending on the nature river channel at the sampling site. A sampler with 2.5 L volume was used to collect water samples over the bridge from non-wade able river sections where the water depth in the river center was greater than 1.5 m. At these sites, the samples were collected from 0.5 m water depth in the center and sides of the channel. Then samples were mixed in the collection and stored in acid-washed 1000 mL polyethylene bottles. For wade able river sections, water samples were collected at the water surface on both sides of the river. Once collected, the water samples were transported to the laboratory at ambient temperature on the same day, then preserved in fridge at 4 °C and they were processed and analyzed within 48 h of collection.

All water samples were split into two before analysis. One part was unfiltered and analyzed for total nitrogen (TN) and total phosphorus (TP). The other part was passed through a 0.45 μm filter, and then the filtrates were analyzed for nitrate nitrogen (NO_3^-–N), ammonium nitrogen (NH_4^+–N), and total soluble phosphate (TDP). All samples were analyzed following the National Standard Methods (Standard Methods for the Examination of Water and Wastewater, 2002) [38]. TN concentrations were measured by alkaline potassium persulfate digestion ultraviolet spectrophotometric method (HJ636-2012) [39], NO_3^-–N concentrations were measured by ultraviolet spectrophotometric method (HJ/T 346-2007) [40], and NH_4^+–N concentrations were measured by Nessler's reagent spectrophotometric method (HJ535-2009) [41]. Total phosphorus (TP) and total dissolved phosphate (TDP) were determined by potassium persulfate digestion ammonium molybdate spectrophotometric method (GB11893-89) [42].

The area of the landscape type was calculated with ArcGIS 12.0 (ESRI, Redlands, CA, USA), and the area of the karst type was measured with AutoCAD 2015 (Autodesk Inc., San Rafael, CA, USA) from 1:100,000 Guilin Karst Hydrogeological Survey maps (Geological Survey Staff, 1991). Statistical analyses were performed using Excel 2015 (Microsoft Corporation, Redmond, WA, USA), IBM SPSS Statistics 25 (IBM Inc., Armonk, NY, USA).

3. Results

3.1. Meteorological and Hydrological Conditions over the Study Period

The precipitation from October 2018 to September 2019 was approximately 2245.8 mm, which was 71.11% more than the 1312.5 mm from October 2017 to September 2018. The precipitation from April to September contributed about 75% of the annual precipitation. Thus, April 2018–September 2018 and April 2019–September 2019 were defined as the wet seasons, while October 2017–March 2018 and October 2018–March 2019 as the dry seasons for the monitoring periods. Overall, there was a distinct seasonal variation in riverine discharges which were greater in the wet season than dry season influenced by rainfall (Figure 2).

In spatial distribution, discharges decreased significantly both at the outlet sections (M_3 and H_4) of tributaries (Mudong River and Huixian River), while increased from upstream to downstream sections of the Xiangsi River main stem basin with greater values than those of tributaries during the same period (Figures 2 and 3). X_2 catchment covers 88.4% of X_3 catchment, and its share of discharge in X_3 section ranged from 64.5% to 96.7% with a mean value of 82.3%. M_3 catchment covers 11.4% of X_3 catchment, and its share of discharge in X_3 section ranged from 1.4% to 34.9% with a mean value of 7.9% during the wet season and 17.3% during the dry season. H_4 catchment (tributary Huixian River sub-basin) covers 34.1% of X_4 catchment, and its share of discharge ranged from 0.2% to 17.4% with a mean value of 6.2%.

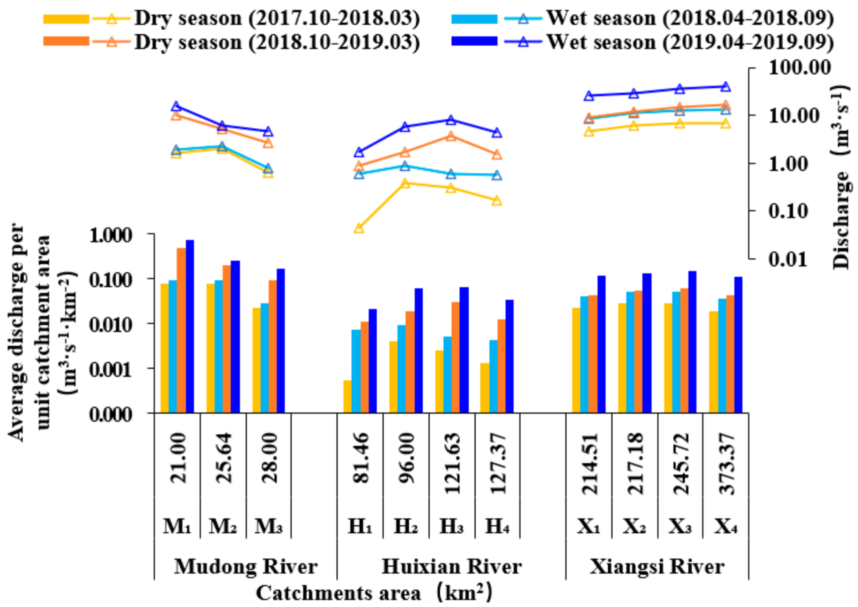

Figure 3. The mean discharge (lines) and discharge per unit catchment area (bars) at the eleven monitoring sections in the dry and wet seasons.

Overall, the mean discharge per unit catchment area in basin of the Xiangsi River main stem ranged between tributaries Mudong River and Huixian River sub-basins. Due to the increased quantity of agricultural water intake from the lower reaches of tributaries Mudong River and Huixian River by damming, discharge decreased in both M_2 and H_4 sections, resulting in the decreases of discharge per unit catchment area of the corresponding catchments (Figure 3).

3.2. Spatio-Temporal Variations of Nutrient Concentration

TN and TP concentrations at each monitoring section are shown in Figure 4. TN and TP concentrations ranged from 0.48~27.55 mg/L and 0.03~2.49 mg/L respectively. Based on the "Chinese Environmental Quality Standards for Surface Water" (GB3838-2002) [43] and the requirements of Guilin Surface Water Environmental Functional Zone Division, TN and TP pollution occur when the concentrations exceed 1.0 mg/L and 0.2 mg/L respectively. As shown in Figure 4, 90.9% and 50.0% of 110 collected water samples in the dry season were categorized as having TN and TP pollution respectively, while 83.6% and 49.2% of 132 collected water samples in the wet season, indicating the more serious pollution of TN than TP in river water. Moreover, 100% and 81.8% of 88 collected water samples in Xiangsi River basin were categorized as having TN and TP pollution respectively, while 72.7% and 39.4% of 66 samples collected in Mudong River sub-basin and 88.6% and 25.0% of 88 samples collected in Huixian River sub-basin, meaning that TN pollution was more serious than TP in the Xiangsi River.

In the main stem Xiangsi River, the concentration of TN and TP showed a decreasing trend with increasing flow, with the highest nutrient concentrations under low flow conditions in the dry season and lower nutrient concentrations under high flow conditions in the wet season. In the tributaries Mudong and Huixian rivers, the trend of TN and TP concentrations with flow was not obvious, and the difference between the dry and wet seasons was also not obvious (Figure 4).

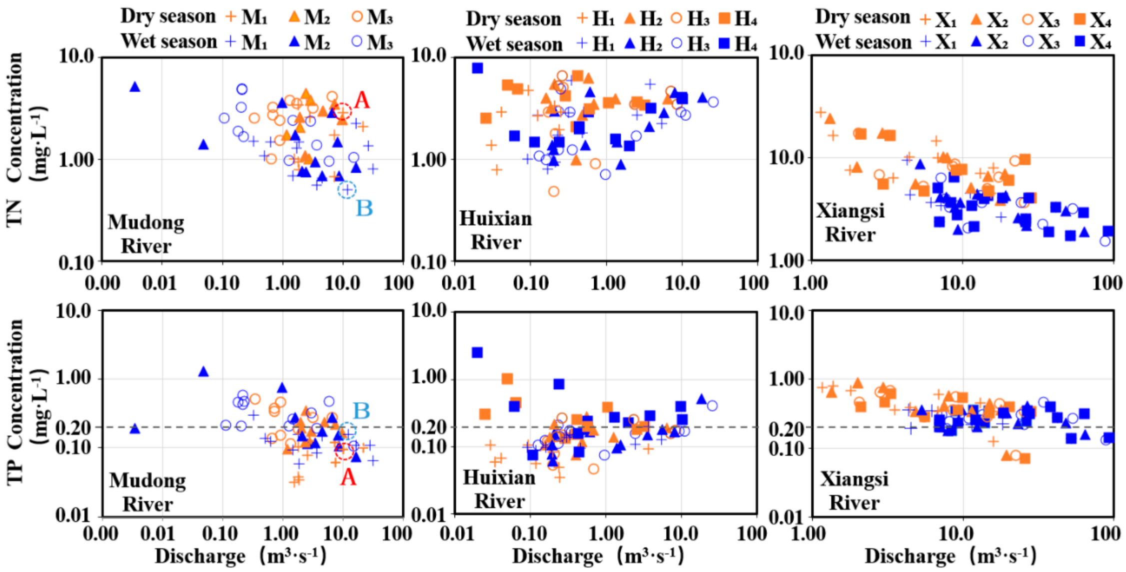

Figure 4. Total nitrogen (TN) and total phosphorus (TP) concentration–discharge relationships at the eleven monitoring sites of three rivers in the dry and wet seasons.

As shown in Figure 5, the mean TN concentration decreased from 3.15~13.10 mg/L (3.15~4.59 mg/L in the wet season) at the upstream X_1 section to 2.58~10.53 mg/L (2.58~3.98 mg/L in the wet season) at the downstream X_4 section of the Xiangsi River, while increased from 1.08~2.01 mg/L (1.08~1.15 mg/L in the wet season) at the upstream M_1 section to 1.90~2.97 mg/L (1.90~2.77 mg/L in the wet season) at the downstream M_3 section in Mudong River, and increased from 1.08~2.01 mg/L (1.08~1.15 mg/L in the wet season) at the upstream H_1 section to 2.40~2.84 mg/L (2.73~2.89 mg/L in the wet season) at the downstream H_4 section in Huixian River. Overall, the range of mean TN concentration in river water of the Huixian karst wetland basin tended to converge to smaller in downstream reaches with values converged from 1.08~13.10 mg/L (1.08~4.59 mg/L in the wet season) at the upstream sections to 1.90~10.83 mg/L (1.90~3.98 mg/L in the wet season) at the downstream sections, especially in the wet season. TP concentration showed the same trend (Figure 5).

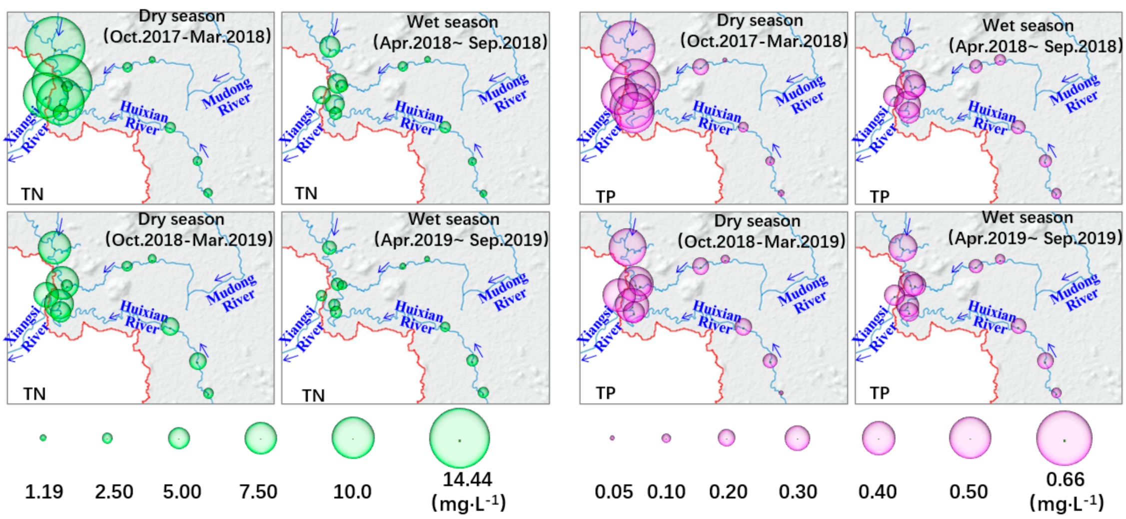

Figure 5. The mean TN and TP concentration at the eleven sampling sites in the dry and wet seasons.

The forms of TN at each monitoring section showed obvious seasonal variations as well as concentration, with NO_3^-–N as the main form in the dry season and the increased contribution of

NH_4^+–N in the wet season. As shown in Figure 6, the mean contribution of NO_3^-–N to TN ranged from 44.8% to 78.3% in the dry season and from 18.2% to 48.0% in the wet season, the mean contribution of NH_4^+–N) to TN in the wet season were 12.9% to 209.8% higher than the mean contribution in the dry season at the eleven monitoring sections. It was also confirmed that the Pearson correlation between NO_3^-–N and $NH_4{}^+$–N was not significant either in the dry season or wet season (Table 2). The mean contribution of TDP to TP ranged from 49.2% to 75.1% in the whole monitoring period at the eleven monitoring sections (Figure 6), so TDP was the main form of TP in different periods, and the correlation between them was more significant in the dry season than wet season (Table 2). The correlations between TN, TP concentrations and discharge were relatively stable at each monitoring section in the Xiangsi River main stem (Table 2).

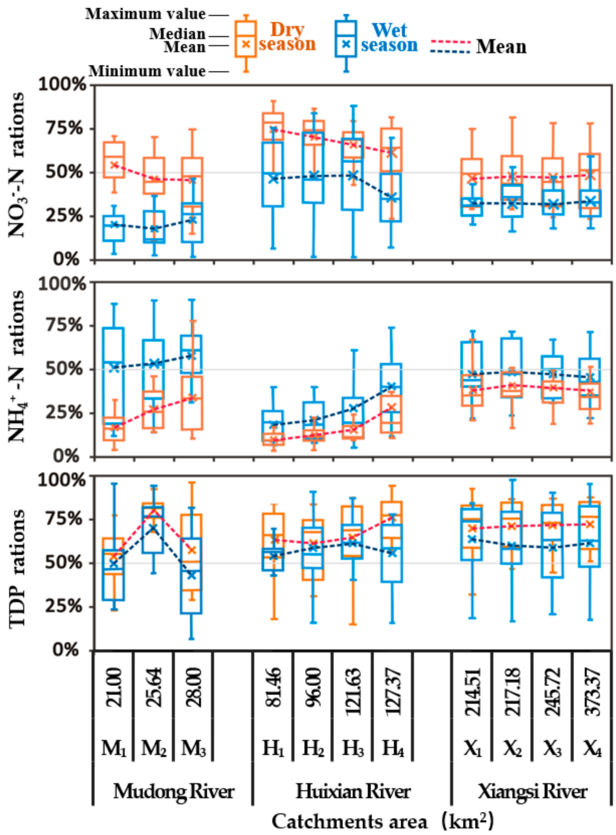

Figure 6. The contribution of NO_3^-–N and NH_4^+–N to TN and of TDP to TP calculated for the sum of all measurements at each station in the dry and wet season.

Table 2. The Pearson correlation coefficient between variables in the dry season (n = 10) and wet season (n = 12).

Variables	Season	Correlation Coefficient										
		M_1	M_2	M_3	H_1	H_2	H_3	H_4	X_1	X_2	X_3	X_4
TN and NO_3^-–N	dry	0.865 **	0.876 **	0.689 *	0.762 **	0.657 *	0.837 **	0.922 **	0.722 **	0.733 **	0.521	0.427
	wet	0.561 *	0.725 **	0.577 *	0.766 **	0.805 **	0.729 **	0.687 **	0.481	0.657 *	0.631 *	0.641 *
TN and NH_4^+–N	dry	0.259	0.630 **	−0.222	0.739 **	0.678 **	0.745 **	0.327	0.756 **	0.825 **	0.855 **	0.805 **
	wet	0.674 **	0.338	0.917 **	0.447	0.476	0.238	0.759 **	0.518 *	0.516 *	0.694 **	0.443
TN and Discharge	dry	0.035	0.228	0.584	0.211	0.035	0.142	−0.201	−0.564	−0.632 *	−0.573	−0.502
	wet	0.039	−0.394	−0.491	0.326	0.580	0.416	0.264	−0.505	−0.490	−0.564	−0.476
NH_4^+–N and NO_3^-–N	dry	0.207	0.492	−0.619	0.166	0.399	0.685 *	−0.346	0.172	0.352	0.226	0.116
	wet	0.170	0.565	0.325	0.415	0.392	−0.025	0.323	0.441	0.311	0.371	0.086
TP and TDP	dry	0.683 *	0.975 **	0.764 **	0.518	0.767 *	0.934 **	0.972 **	0.989 **	0.989 **	0.980 **	0.963 **
	wet	0.335	−0.033	0.499	0.850 **	0.946 **	0.948 **	0.810 **	0.361	0.227	0.426	0.455
TP and TN	dry	0.205	0.813 **	0.048	0.325	0.876 **	0.784 **	0.451	0.574	0.547	0.417	0.315
	wet	0.130	0.215	0.430	0.547	0.565	0.410	−0.086	0.397	0.329	0.111	0.094
TP and Discharge	dry	0.374	0.060	−0.140	0.242	0.172	0.255	−0.345	−0.735 *	−0.776 *	−0.637 *	−0.518 *
	wet	−0.352	−0.463	−0.433	0.311	0.907 **	0.856 **	0.059	−0.475	−0.442	−0.435	−0.402

Note: * means significance level ($p < 0.05$) (significant correlation): ** means significance level ($p < 0.01$) (highly significant correlation).

3.3. Spatio-Temporal Variations of Nutrient Fluxes

Nutrient fluxes (g·s^{-1}) in the rivers were estimated by combining measured nutrient concentration data (mg·L^{-1}) with observed discharges data (m^3·s^{-1}). Figure 7 shows TN and TP fluxes for each spatial catchment scale in the dry and wet seasons. Nutrient fluxes showed significant seasonal variations, with greater fluxes in the wet season than dry season during the same period, which was not consistent with the seasonal variations of nutrient concentration. Nutrient fluxes of the Xiangsi River were the largest among the three rivers and tended to increase from the upstream to downstream, while decrease at the outlet of the Mudong River and Huixian River sub-basin, which was also not consistent with the spatial variations of nutrient concentration. Results suggested that the seasonal variations of nutrient fluxes were mainly controlled by hydrological conditions.

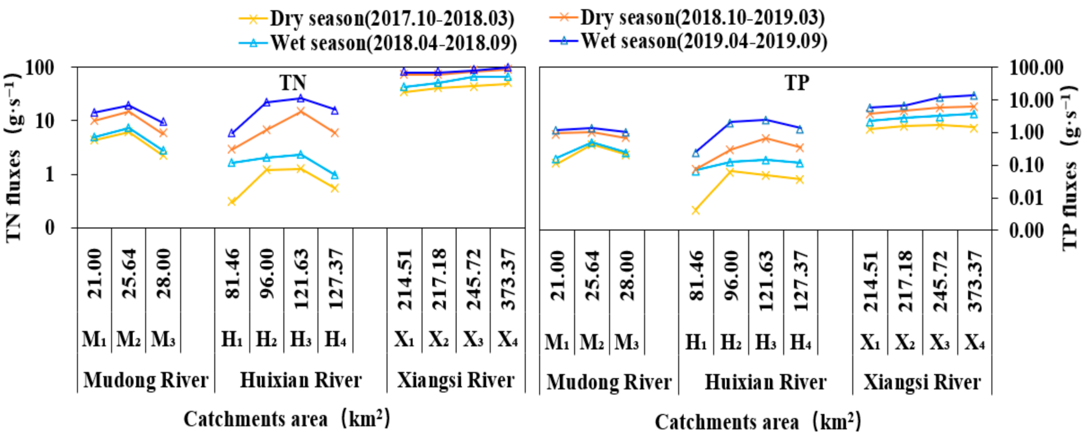

Figure 7. The average TN and TP fluxes at the eleven catchment scales in the dry and wet seasons.

The Person correlation analysis also confirmed that there was a significant positive relation between TN, TP fluxes and discharge at different spatial catchment scales (Table 3). The power function relationships between TN, TP fluxes and discharges at different spatial catchment scales of the three rivers were verified further using regression analysis. Regression models were developed using TN and TP fluxes (g·s^{-1}) as a dependent variable and observed discharge (m^3·s^{-1}) as an explanatory variable. Six models all had significant power function relationships which were maintained not only in different periods (dry and wet seasons) but also in different hydrological years with different rainfall frequencies (Figure 8), further indicating that hydrological conditions played a dominant role in nitrogen and phosphorus nutrient fluxes in river water.

Table 3. The Pearson correlation coefficient between discharge and TN, TP fluxes of the 11 catchment scales.

Variable		Correlation Coefficient										
		M_1	M_2	M_3	H_1	H_2	H_3	H_4	X_1	X_2	X_3	X_4
Discharge	TN flux	0.837 **	0.660 *	0.741 **	0.910 **	0.990 **	0.976 *	0.992 *	0.669 **	0.746 **	0.660 **	0.739 **
	TP flux	0.937 **	0.733 **	0.752 **	0.949 **	0.933 **	0.945 **	0.964 **	0.842 **	0.832 **	0.675 **	0.727 **

Note: * means significance level ($p < 0.05$) (significant correlation): ** means significance level ($p < 0.01$) (highly significant correlation).

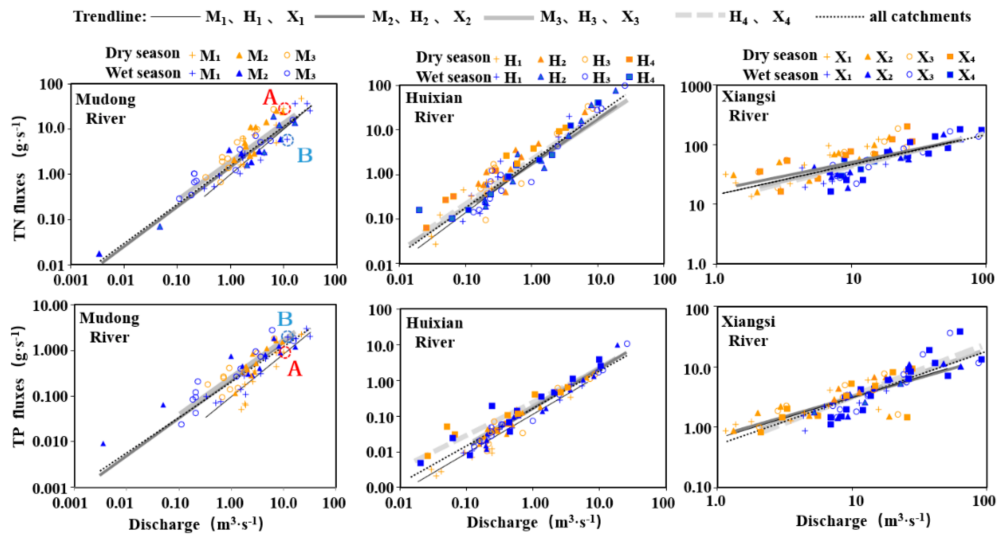

Figure 8. The relation between discharge and TN or TP fluxes of the eleven catchment scales for the three rivers in the dry and wet seasons.

TN and TP fluxes of the upstream catchment can be calculated by these power function equations (Table 4) based on the observed discharge at the catchment outlet. Table 5 shows the relative contributions of area, discharge, and nutrient flux in the upstream X_2, M_3, H_4 catchments to the downstream X_3 and X_4 catchments. In M_3 upstream catchment (tributaries Mutong River sub-basin) which covered 11.4% of X_3 catchment, the share of TN and TP fluxes ranged between 5.5% and 8.9%, and in H_4 upstream catchment (tributaries Huixian River sub-basin) which covered 34.1% of X_4 catchment, the share of TN and TP fluxes ranged between 3.7% and 6.1%, which were both less than the contribution of area and discharge in the dry and wet seasons respectively. Therefore, TN and TP fluxes in the lower reaches of the Xiangsi River mainly came from the upper X_2 catchment, which confirmed the more serious nitrogen and phosphorus pollution in the upper reaches of the Xiangsi River.

Table 4. Regression analysis results for discharge as a function of TN and TP fluxes at the 11 catchment scales.

TN					TP				
Catchments	**N (Number of Samples)**	**a**	**b**	**R^2**	**Catchments**	**N**	**a**	**b**	**R^2**
M_1	22	1.2796	0.9942	0.8166	M_1	22	0.979	0.9549	0.8383
M_2	22	1.8676	0.8820	0.8715	M_2	22	0.2161	0.8436	0.8722
M_3	22	2.2977	0.8456	0.8487	M_3	22	0.2797	0.8307	0.8267
Mudong River	66	1.8579	0.8554	0.8426	Mudong River	66	0.1954	0.7791	0.7749
H_1	22	2.6887	1.1616	0.9092	H_1	22	0.1104	1.1109	0.9463
H_3	22	2.5794	1.0961	0.8763	H_3	22	0.1484	1.1794	0.9471
H_4	22	2.3225	1.1149	0.8779	H_4	22	0.1450	1.1344	0.9479
H_5	22	2.9005	0.9779	0.9252	H_5	22	0.2435	0.9535	0.8846
Huixian River	88	2.5035	1.0610	0.8972	Huixian River	88	0.1517	1.0629	0.8767
X_1	22	16.082	0.4885	0.5212	X_1	22	0.6286	0.6731	0.7427
X_2	22	17.104	0.4679	0.5131	X_2	22	0.7229	0.6384	0.6375
X_3	22	15.686	0.5123	0.5360	X_3	22	0.5347	0.7834	0.6671
X_4	22	13.852	0.5650	0.5860	X_4	22	0.4476	0.8461	0.6935
Xiangsi River	88	15.996	0.5016	0.5270	Xiangsi River	88	0.5580	0.7548	0.7115

Table 5. The relative contribution of area, discharge and nutrient flux in the upstream X_2, M_3, H_4 catchments to the downstream X_3 and X_4 catchments.

Catchments			Contribution (%)				Mean (Min–Max)	
			Discharge		TN Fluxes		TP Fluxes	
Down-Stream	Upstream	Area	Dry Season	Wet Season	Dry Season	Wet Season	Dry Season	Wet Season
X_3	X_2	88.4	80.3 (64.5–92.9)	88.5 (67.8–96.7)	92.5 (69.4–99.3)	91.5 (69.4–99.2)	91.0 (77.1–97.8)	89.8 (31.4–99.0)
X_3	M_3	11.4	17.3 (6.5–34.9)	7.9 (1.4–20.8)	7.2 (1.6–23.0)	5.5 (1.1–12.0)	8.9 (4.3–24.8)	7.5 (2.5–17.8)
X_4	H_4	34.1	6.3 (0.8–13.3)	6.2 (0.2–17.4)	3.7 (0.1–10.0)	6.1 (0.3–22.7)	3.9 (0.4–7.5)	6.0 (1.6–19.8)

Nutrient export coefficients (g·km^{-2}·s^{-1}) are estimates of the nutrient fluxes (g·s^{-1}) normalized by area (km^2). As shown in Figure 9, the mean nutrient export coefficients of TN and TP in tributary Mudong River sub-basin were generally larger than those in Huixian River sub-basin during the same season, and those in the Xiangsi River basin were estimated between them.

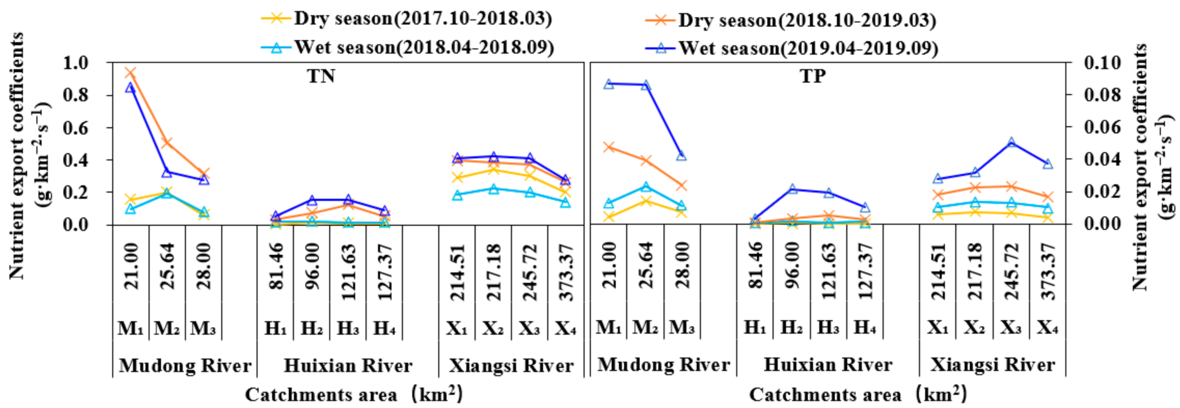

Figure 9. The mean nutrient export coefficients of TN and TP for the eleven catchment scales in the dry and wet seasons.

Since nutrient fluxes at different spatial catchment scales were significantly positively correlated with discharges in this study, the nutrient export coefficients were significantly positively correlated with discharges per unit area accordingly ($p \leq 0.05$, correlation coefficient ranged from 0.569 to 0.953). The mean nutrient export coefficients of TN and TP were significantly positively correlated with the share of agricultural land and covered karst land over the monitoring periods (Table 6). The spatial variations of TN and TP fluxes at small catchment scales in tributaries Mudong River and Huixian River sub-basin were greater than that at large catchment scales in the Xiangsi River main stem (Table 7).

Table 6. The Pearson correlation coefficient between the average nutrient export coefficients and the share of agricultural land in the dry seasons and wet seasons.

Variable	Average TN Flux Export Coefficients				Average TP Flux Export Coefficients			
	Dry Season (2017.10–2018.3)	Wet Season (2018.4–2018.9)	Dry Season (2018.10–2019.3)	Wet Season (2019.4–2019.9)	Dry Season (2017.10–2018.3)	Wet Season (2018.4–2018.9)	Dry Season (2018.10–2019.3)	Wet Season (2019.4–2019.9)
Share of agricultural land (%)	0.844 **	0.756 *	0.769 **	0.772 **	0.703 *	0.647 *	0.938 **	0.840 **
Share of covered karst land (%)	0.841 **	0.728 *	0.748 *	0.725 *	0.728 *	0.607 *	0.906 **	0.760 **

Note: * means significance level ($p < 0.05$) (significant correlation); ** means significance level ($p < 0.01$) (highly significant correlation).

Table 7. The significant value of discharge, TN and TP flux variation within the three investigated rivers calculated using the one-way ANOVA.

Variable	Significant Value		
	Mudong River (M_1, M_2, M_3)	**Huixian River (H_1, H_2, H_3, H_4)**	**Xiangsi River (X_1, X_2, X_3, X_4)**
Discharge	0.023	0.256	0.496
TN flux	0.115	0.303	0.394
TP flux	0.281	0.481	0.646

Note: The smaller the significant value, the greater the spatial differentiation.

4. Discussion

4.1. Spatio-Temporal Variations of Riverine Nutrient Controlled by Hydrological Conditions

Analysis revealed that NO_3^-–N was the main form of TN in the dry season and the contribution of NH_4^+–N to TN increased in the wet season. In the dry season, because of the reduced discharge and slow flow of rivers, NO_3^-–N was easily transformed from NH_4^+–N in human and animal manure sewage drained into the rivers, which was soluble in water and does not easily adsorb to sediment, and could be transported to surface water through various pathways (including surface runoff, subsurface seepage and groundwater recharge) [44,45], ultimately becoming the main form of riverine TN. In the wet season, because of the fertilization and irrigation of agricultural land and the conditions of weak nitrification and abundance available nitrogen, excess NH_4^+–N which above the soil's adsorption capacity was carried by plenty of surface runoff directly flowing into the river water or infiltrating from the soil to groundwater and ultimately recharging to surface rivers, directly or indirectly lead to an increase in the contribution of NH_4^+–N to TN in rivers. Thus, the seasonal hydrological conditions played a controlling role in determining the contributions of NO_3^-–N and NH_4^+–N to TN.

Hydrological processes of rainfall-runoff in surface play an important role in nitrogen and phosphorus transfer in the basin. Large amounts of suspended and adsorbed nutrients are transported to the river when runoff increases caused by rainfall [46,47], especially phosphorus, as TP is mainly carried by surface runoff in the forms of dissolved material and suspended particulate. In this study, TDP was the main form of TP at different spatial catchment scales in dry and wet seasons. Although the mean contribution of TDP to TP in the dry season was higher than wet season, the contribution of TDP to TP was not significant in seasonal disparities because our study did not target rainfall events, periods of high flow are underrepresented in our assessment. Analysis showed that the correlation between TP and TDP was more significant in the dry season than the wet season, and was most significant in Huixian River than other two rivers (Table 2). This may be mostly explained by hydrological conditions with lower-flow and slower flow velocity during the dry season as well as in Huixian River, helping to enhance the correlations between TP and TDP. Altering flow conditions by damming Mudong River and Huixian River for water storage may also result in reduced particulate phosphorus (PP) fluxes. High flow conditions during the wet season increase the proportion of PP in TP and re-suspend the sediments stored at the river bed, providing an additional potential for P release.

The controlling of hydrological conditions on the nutrient export in Huixian karst wetland rivers not only in terms of the different forms of TN and TP, but also in terms of concentration and flux. The results in this study show that the riverine nutrient concentrations were generally higher under low-flow conditions, while fluxes were relatively higher under high flow conditions during the wet season, indicating that the controlling of hydrological conditions on the nutrient export was stronger than other factors. Thus, TN, TP concentrations and fluxes in the Xiangsi River showed significant seasonal variations as discharge, benefited from the significant correlation with discharge (Table 3). The role of hydrological conditions in controlling nitrogen and phosphorus export in surface water systems has been verified in several studies [48,49]. In our study, the TN and TP fluxes of the upstream catchment can be calculated by power function equations (Table 4). Similar empirical equations have been presented in other areas of China, showing a significant exponential or logarithmic relationship between nutrient fluxes and discharges [50,51]. However, since riverine nitrogen and phosphorus are related to various factors such as natural attributes and human activities in the study area, there are regional limitations of the empirical equations presented in each study area. Therefore, the empirical equations proposed in our study are only applicable to similar basins.

4.2. Spatio-Temporal Variations of Riverine Nutrient Affected by Human Activities

It is generally accepted that human-influenced landscapes such as urban and agricultural land are nutrient sources in river water [52,53]. The correlation between nutrient concentrations and discharges was not significant in the sub-basins of tributaries Mudong River and Huixian River, where agriculture was the main type of landscape in addition to forest (Table 1), so the rivers were mainly polluted by nitrogen and phosphorus from agricultural non-point sources. The sewage from poultry, aquaculture farming and living drained nitrogen and phosphorus pollutants into river water in the dry season, and the application of fertilizers increased augmenting nitrogen and phosphorus pollution in the wet season [32]. Seasonal variations in nitrogen sources caused by human activities in the Mudong River and Huixian River sub-basins, resulted in the difference in TN concentrations (observation A and B in Figure 4) and fluxes (observation A and B in Figure 8) for the similar flow conditions after rain events in the dry season (observation A in Figure 2) or during low-flow period in the wet season (observation B in Figure 2). It is also confirmed by the disparities in the contribution ratios between NO_3^-–N and NH_4^+–N in the wet and dry seasons (Figure 6). In this study, the contributions of NO_3^-–N to TN were generally greater than 50% in the dry seasons (the contributions of NO_3^-–N was 68.7% at observation A in Figure 4, while NH_4^+–N was only 9.7%), and NH_4^+–N were generally greater than 50% in the wet seasons (the contributions of NH_4^+–N to TN was 89.5% at observation B in Figure 4, while NO_3^-–N was only 7.0%). Among the three rivers, TN and TP pollution of the Xiangsi River was the most serious, with the nutrient pollution mainly coming from the X_2 upstream catchment, where urban was the main landscape type (Table 1), so the Xiangsi River was mainly affected by nitrogen and phosphorus point source pollution. In X_1 and X_2 sections, the nutrient concentrations were high and the discharge-concentration relationships (Figure 4) were likely to display dilution pattern [54] due to the stationary source with large and stable discharge of sewage drained from urban residential and industrial activities.

In the Xiangsi River main stem, TN and TP fluxes increased with increasing catchment area scale, while in M_3 and H_4 sections, the tributaries outlets of Mudong River and Huixian River, TN and TP fluxes decreased when compared with that of upstream catchments. Discharge was the dominant factor since the nutrient fluxes were positively correlated with it. The decrease in discharge is due to the damming of water by agricultural producers. However, since TN and TP fluxes in the lower reaches of the Xiangsi River mainly came from the X_2 upstream catchment (Table 5), the decreased quantity of water flowing from tributaries had less impact on TN and TP fluxes in the Xiangsi River main stem, indicating that the spatial variations of TN and TP fluxes at small catchment scales in lower-order tributaries were larger than that at large catchment scales in higher-order main stem, due to the human activities in sub-basin.

4.3. Spatio-Temporal Variations of Riverine Nutrient Restricted by Karst Features

It is generally accepted that there is a strong positive correlation between nutrient export and the proportion of available and arable land within a catchment [55]. This was confirmed also in this study that there was a significant positive correlation between the mean nutrient export coefficients and the share of agricultural land in each catchment area over different periods (Table 6). Further studies indicated that the share of covered karsts was significantly positively correlated with the mean of nutrient export coefficients as well as the share of agricultural land in each catchment area (Figure 10), with the correlation coefficients of 0.837 and 0.976, respectively. In karst region, bare-karst areas are extremely difficult to exploit within no or little soil which is thin, patchy, and slow to form, while cover-karst areas are usually the central and areas for intensive human living and productive activities, as well as the runoff-drainage areas of catchments. As a result, catchment with high shares of cover-karst area are generally characterized by high shares of agricultural land, high discharge per unit area, and correspondingly high TN, TP nutrient export coefficients.

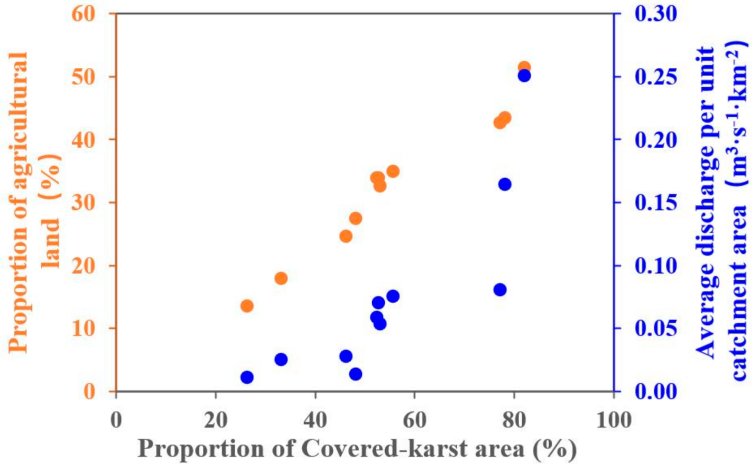

Figure 10. Scatter plots of the relation between the proportion of covered-karst and agricultural land, the average discharge per unit area.

In addition to constraining the share of available and arable land within the catchment that indirectly affect the nitrogen and phosphorus flux, karst features also have strong control on water movement within the catchment and indirectly affect nitrogen and phosphorus concentrations in surface water systems, causing the range of mean TN and TP concentrations at the outlet of each catchment to converge to smaller in downstream reaches during the same season (Figure 5). The aquifer of the Huixian karst wetland basin is characterized by the high altitude and impermeable non-karst aquifers in the north and south, and karst water storage tectonic basin in the central lowland (Figure 11). The tectonic basin receives precipitation and surface water recharge from the oblique flanks, as well as recharge from upstream or adjacent karst groundwater, and from external sources (e.g., Qingshitang Reservoir water). The main drainage directions of surface water and groundwater systems flow from the north and south to the central tectonic lowlands, and these surface water and groundwater have rapidly influenced the development of the central karst landscape, developing and forming numerous wetland lakes and swamps—Huixian karst wetland, where the unique hydrogeology is characterized by primarily decentralization runoff with slow flow exchanging between surface water and groundwater in the central tectonic lowlands. In downstream reaches of three rivers, a rising groundwater table can intersect the near-river catchment surface, especially in heavy rainfall events during the wet season, when the river level raised so high that the lowlands were almost inundated and the range of nutrient concentrations converged to smaller for the connections of all the surface water. With the increasing catchment scale, the hydraulic connections were stronger in the confluent area of the lower reaches of three rivers, suggested that the effect of hydrological connectivity formed under the hydrogeological constraints of karst on nutrient concentrations prevails over the effect of other factors, especially in the wet season. This convergence effect is common in ecological data and depends on the spatial scale of observation [56] and hydrological characteristics of basin. Identification of the effects of karst features on nutrient export may not be possible without complete understanding of the restrictive relation between karst features and hydrological conditions, as well as landscape which was closely related to human activities in basin.

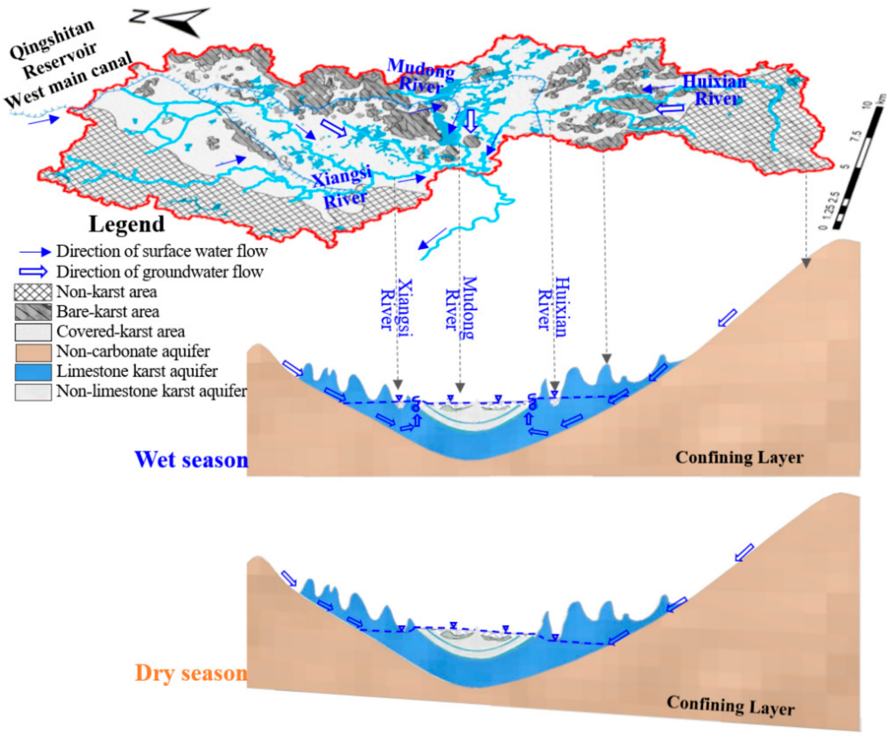

Figure 11. The interaction and conversion relationship of surface–underground water during wet season and dry season in Huixian karst wetland.

4.4. Measures to Control Nitrogen and Phosphorus Pollution in Karst River Waters

Results from riverine nutrients monitoring for the whole study period show that the situation of nitrogen and phosphorus in the rivers of the Huixian karst wetland was not optimistic. TN and TP concentrations were wider than the observed values in other karst systems in Europe, North America and southwest China, higher than those in other wetland systems and in rivers of Lijiang River basin (Table 8), indicating the high concentrations of TN and TP in the rivers of study area. During the wet season, when nitrogen and phosphorus concentrations were relatively low, up to 83.6% and 49.2% of water samples were still categorized as having TN and TP pollution, respectively, even in the wet season when the nitrogen and phosphorus concentrations were relatively lower. The complexity of the dual surface–subsurface hydrological structure of the Huixian karst wetland basin means that diffuse nutrient pollution is particularly difficult to control. Complex relationships between nutrient sources, forms and transfer in river waters also mean the necessity of long-term implementation of various measures. Temporality and spatiality must be taken into account together in setting and implementing measures for providing measures to control nitrogen and phosphorus diffuse pollution. This implies that, when solving water quality problems on the local scale, we should focus on the effects of catchment-scale variables, such as land use mainly affected by human activities or hydrogeological features on river water quality from a long-term perspective [24,57].

Table 8. Range of observed concentration of TN and TP in other karstic systems, wetland systems and rivers in Lijiang River basin.

Water Sample Belonging to		Range of Concentration Values (mg/L) TN	TP	Monitoring Time	Source
Karstic system	Gort Lowlands catchment (west of Ireland)	0.0~3.9	0.0037~0.121	March 2010–March 2013	[28]
	Spring Creek watershed (northeastern USA)	≤3.0	≤0.25	January 2004–October 2014	[58]
	Karst catchment in Shuangqing village (Guizhou, China)	0.99~5.72	0.03~1.01	May 2015–April 2016	[59]
Wetland system	Natural wetlands in the Toenepi catchment (New Zealand)	0.235~13.5	0.00533~1.64	(TN) October 2011 and September 2013; (TP) March 1995–April 1997	[60,61]
	Chapel Branch Creek watershed (South Carolina)	≤4.3	≤1.65	2007–2009	[27]
	Luoshi River Wetland (Yunnan, China)	0.6~3.4	0.04~0.15	January 2014–May 2014	[62]
Lijiang River basin	Jingui River (The tributary of the Lijiang River)	0.64~8.91	0.03~0.75	October 2016–October 2017	[63]
	Stream in Gan village (The tributary of the Lijiang River)	0.86~9.36	0.02~0.14	November 2013–November 2014	[64]
	The main stem	0.44~5.56	0.002~0.49	September 2012–September 2013	

In our study, results demonstrated that high concentrations of nitrogen and phosphorus in the river generally occurred during low flows, which were consistent with the findings of others that nitrogen and phosphorus were retained within the river during low flows [65,66]. More precipitation and thus more water discharge can dilute the nutrients in the water of the mainstem Xiangsi River, then reduce the nutrient concentrations. However, the nutrient concentrations can also increase in the tributaries Mudong and Huixian River, namely when nutrients are washed out or when wastewater tanks overflow. Results confirmed that human-influenced land-use types such as urban and agricultural land are nutrient sources [52,53]. Since the current situation of nutrient pollutions in Xiangsi River basin was mainly contributed from the upstream urban dominant catchment, with 100% and 81.8% of 88 collected water samples being categorized as having TN and TP pollution respectively. Therefore, in terms of setting up river nitrogen and phosphorus monitoring stations, it is more reasonable for the monitoring stations of the mainstem Xiangsi River to be close to the downstream of the urban outfall, mainly to monitor the point source of pollution in urban areas. The monitoring station for comparison and reference should be set up in the upstream of the urban area. The monitoring stations of tributaries Mudong River and Huixian River are more reasonable setting at downstream of irrigation canals, farms and domestic sewage outfalls, to focus on monitoring agricultural nitrogen and phosphorus pollution. Additionallly, with regard to nitrogen and phosphorus pollution control measures, some measures of restricting during agricultural water peak in the wet season or recharging during low flows in the dry season are necessary, to maintain ecological flows in the river and to reduce the frequency of high concentrations of nitrogen and phosphorus. It is clear that policy measures should be taken as soon as possible by the local government to limit the nutrient pollution emissions from the upstream Lingui District for reducing the nitrogen and phosphorus of the lower reaches. For agricultural land, ecological farming with central collection of aquaculture wastewater and treatment before discharge, and ecological cultivation with environmentally friendly fertilization should be advocated and supported by local managers to reduce agricultural nitrogen and phosphorus pollution.

5. Conclusions

The nutrient concentration and forms within 11 nested catchments ranging in scale from 21.00 km^2 up to a maximum of 373.37 km^2 in Huixian karst wetland have been monitored over 2 years (from October 2017 to September 2019) to identify the spatial and temporal variations of riverine nutrients affected by hydrological conditions, human activities and karst features. The following conclusions can be made based on the results of this study:

(1) In the dry season, NO_3^-–N was the main form of TN with a mean contribution ranged from 44.8% to 78.3% at the eleven monitoring sections, while in the wet season, the mean contribution of NH_4^+–N to TN were 12.9% to 209.8% higher than dry season. TDP was the main form of TP in different periods with a mean contribution ranged from 49.2% to 75.1% in the whole monitoring period and a more significant correlation between them in the dry season than the wet season. The concentrations of TN and TP were generally higher during low flow, while the fluxes were higher during high flow events in the wet season and maintained a power function relationship with discharges over the sampling periods. Results demonstrated the seasonal hydrological condition was a decisive factor controlling the seasonal variations of in-stream TN and TP.

(2) The different nitrogen and phosphorus sources from human activities in different spatial catchments induced dynamic disparities of riverine nitrogen and phosphorus. In agriculturally dominant catchments of tributaries Mudong and Huixian River, the forms, concentrations, and fluxes of TN and TP were different even if the discharge from the same monitoring section was the same in different seasons. While in urban dominant catchments of the Xiangsi River main stem, the nutrient concentrations were generally higher (up to 100% and 81.8% of water samples were categorized as having TN and TP pollution, respectively) and maintained a relatively stable correlation with discharge over the sampling periods (the Pearson correlation coefficient between discharge and TN, TP concentration were −0.476~−0.632 and −0.402~−0.776, respectively). On the other hand, the significant values of discharge, TN and TP flux in Xiangsi River (0.496, 0.394, 0.646, respectively) were larger than that in tributaries Mudong River (0.023, 0.115, 0.281, respectively) and Huixian River (0.256, 0.303, 0.481, respectively), indicating that the spatial variations of TN and TP fluxes were larger at small catchment scales in lower-order tributaries than that at large catchment scales in higher-order main stem for the increased quantity of agricultural water taking from tributaries. These results suggested that the catchment-scale human activities play an important role in inducing spatial disparities in riverine nitrogen and phosphorus.

(3) There was a significant positive correlation between the share of covered karst land and the mean TN and TP nutrient export coefficients ($p \leq 0.05$, the correlation coefficient ranged from 0.607 to 0.906). Because of the dispersed discharge of hydrological system in Huixian Karst Wetland basin, the range of mean TN and TP concentrations in different rivers tended to convergence to smaller in downstream reaches, especially in the wet season. The results demonstrated that karst features had a strong constraint on the spatial scale similarity of riverine nitrogen and phosphorus.

In addition, based on the spatial and temporal variations of nitrogen and phosphorus in river waters influenced by hydrological conditions, human activities and karst features, corresponding scientific suggestions have been proposed to control nitrogen and phosphorus pollution of the water system in Huixian Karst Wetland basin.

Clearly, our understanding of the links between hydrological conditions, human activities, karst features, and spatio-temporal dynamics of riverine nitrogen and phosphorus in Huixian basin is relatively restricted. For example, resource constraints dictate that this study has just focused on TN and TP in river waters at different catchment scales that are relatively easy to measure. However, nitrogen and phosphorus transfer in the surface water is just one aspect of nutrient cycling in the water system. A fuller understanding of nutrients transfer at different vertical depths is required, as river waters, soil, and groundwater are all the mediums in which nutrients flow, especially in a karst-affected basin where surface-water and groundwater are closely linked. Thus, linking the study of water cycling with the analysis of nutrient transfer processes will be an important aspect of nitrogen and phosphorus spatio-temporal variations research in Huixian karst wetland basin for further research.

Author Contributions: Investigation and sampling, L.P., Z.W. (Zhiqiang Wu), Z.W. (Zupeng Wan), Z.Z., J.H. and Z.L.; data curation, X.X.; resources, B.X.; writing—original draft preparation, L.P., J.D. and X.W.; supervision, X.W.; project administration, J.D. All authors have read and agreed to the published version of the manuscript.

Funding: This research was funded by the National Natural Science Foundation of China (No. 51979046, No. 51569007), and the Natural Science Foundation of Guangxi Province, China (Grant No. 2018GXNSFAA294087, No. 2018GXNSFAA050022).

Conflicts of Interest: The authors declare no conflict of interest.

References

1. Anderson, D.M.; Glibert, P.M.; Burkholder, J.M. Harmful algal blooms and eutrophication: Nutrient sources, composition, and consequences. *Estuaries* **2002**, *25*, 704–726. [CrossRef]
2. Withers, P.J.A.; Neal, C.; Jarvie, H.P.; Doody, D.G. Agriculture and eutrophication: Where do we go from here? *Sustainability* **2014**, *6*, 5853–5875. [CrossRef]
3. Gruber, N.; Galloway, J.N. An Earth-system perspective of the global nitrogen cycle. *Nature* **2008**, *451*, 293–296. [CrossRef] [PubMed]
4. Elser, J.; Bennett, E. Phosphorus cycle: A broken biogeochemical cycle. *Nature* **2011**, *478*, 29–31. [CrossRef]
5. Liu, C.Q.; Lang, Y.C.; Li, S.L.; He, C.P.; Tu, C.L.; Liu, T.Z.; Wei, Z. Researches on biogeochemical processes and nutrient cycling in karstic ecological systems, southwest China: A review. *Earth Sci. Front.* **2009**, *16*, 1–12. (In Chinese)
6. Bakalowicz, M. Karst groundwater: A challenge for new resources. *Hydrogeol. J.* **2005**, *13*, 148–160. [CrossRef]
7. Bai, X.Y.; Wang, S.J.; Xiong, K.N. Assessing spatial–temporal evolution processes of karst rocky desertification land: Indications for restoration strategies. *Land Degrad. Dev.* **2013**, *24*, 47–56. [CrossRef]
8. Ford, D.; Williams, P.D. *Karst Hydrogeology and Geomorphology*; John Wiley & Sons Ltd.: Chichester, UK, 2007.
9. Buckerfield, S.J.; Waldron, S.; Quilliam, R.S.; Naylor, L.; Li, S.L.; Oliver, D.M. How can we improve understanding of faecal indicator dynamics in karst systems under changing climatic, population, and land use stressors?–Research opportunities in SW China. *Sci. Total Environ.* **2019**, *646*, 438–447. [CrossRef]
10. Coxon, C. Agriculture and Karst. In *Karst Management*; Van Beynen, P., Ed.; Springer: Dordrecht, The Netherlands, 2011; pp. 103–138.
11. Jiang, Y.J.; Wu, Y.X.; Yuan, D.X. Human impacts on karst groundwater contamination deduced by coupled nitrogen with strontium isotopes in the Nandong underground river system in Yunan, China. *Environ. Sci. Technol.* **2009**, *43*, 7676–7683. [CrossRef]
12. Hartmann, A.; Goldscheider, N.; Wagener, T.; Lange, J.; Weiler, M. Karst water resources in a changing world: Review of hydrological modeling approaches. *Rev. Geophys.* **2014**, *52*, 218–242. [CrossRef]
13. Bloom, A.L. Water-formed structures: Geomorphology and hydrology of karst terrains. *Science* **1989**, *243*, 1618–1619. [CrossRef] [PubMed]
14. Einsiedl, F.; Maloszewski, P.; Stichler, W. Multiple isotope approach to the determination of the natural attenuation potential of a high-alpine karst system. *J. Hydrol.* **2009**, *365*, 113–121. [CrossRef]
15. Katz, B.G.; Bohlke, J.K.; Hornsby, H.D. Timescales for nitrate contamination of spring waters, northern Florida, USA. *Chem. Geol.* **2001**, *179*, 167–186. [CrossRef]
16. Sinha, E.; Michalak, A.M.; Balaji, V. Eutrophication will increase during the 21st century as a result of precipitation changes. *Science* **2017**, *357*, 405–408. [CrossRef]
17. Blaen, P.J.; Khamis, K.; Lloyd, C.E.M.; Bradley, C.; Hannah, D.; Krause, S. Real-time monitoring of nutrients and dissolved organic matter in rivers: Capturing event dynamics, technological opportunities and future directions. *Sci. Total Environ.* **2016**, *569*, 647–660. [CrossRef]
18. Manzoni, S.; Porporato, A. Common hydrologic and biogeochemical controls along the soil-stream continuum. *Hydrol. Process.* **2011**, *25*, 1355–1360. [CrossRef]
19. Ahearn, D.S.; Sheibley, R.W.; Dahlgren, R.A.; Anderson, M.; Johnson, J.; Tate, K.W. Land use and land cover influence on water quality in the last free-flowing river draining the western Sierra Nevada, California. *J. Hydrol.* **2005**, *313*, 234–247. [CrossRef]
20. Dupas, R.; Musolff, A.; Jawitz, J.W.; Rao, P.S.C.; Jager, C.G.; Fleckenstein, J.H.; Rode, M.; Borchardt, D. Carbon and nutrient export regimes from headwater catchments to downstream reaches. *Biogeosciences* **2017**, *14*, 4391–4407. [CrossRef]

21. Tiwari, T.; Lidman, F.; Laudon, H.; Lidberg, W.; Agren, A.M. GIS-based prediction of stream chemistry using landscape composition, wet areas, and hydrological flow pathways. *J. Geophys. Res. Biogeosci.* **2017**, *122*, 65–79. [CrossRef]
22. Zahra, T.; Abbott, B.W.; Olivier, T.; Jacques, B.; Gilles, P. Proximate and ultimate controls on carbon and nutrient dynamics of small agricultural catchments. *Biogeosciences* **2015**, *12*, 15337–15367.
23. Aitkenhead-Peterson, J.A.; Steele, M.K. Dissolved organic carbon and dissolved organic nitrogen concentrations and exports upstream and downstream of the Dallas–Fort Worth metropolis, Texas, USA. *Mar. Freshw. Res.* **2016**, *67*, 1326–1337. [CrossRef]
24. Cui, L.; Li, W.; Gao, C.; Zhang, M.; Zhao, X.; Yang, Z.; Lei, Y.R.; Di, H.; Wu, M. Identifying the influence factors at multiple scales on river water chemistry in the Tiaoxi Basin, China. *Ecol. Indic.* **2018**, *92*, 228–238. [CrossRef]
25. Sterner, R.W.; Elser, J.J. *Ecological Stoichiometry: The Biology of Elements from Molecules to the Biosphere*; Princeton University Press: Princeton, NJ, USA, 2002.
26. Gao, Y.; Yu, G.R. Biogeochemical cycle and its hydrological coupling processes and associative controlling mechanism in a watershed. *Acta Geogr. Sin.* **2018**, *73*, 1–13. (In Chinese)
27. Williams, T.M.; Amatya, D.M.; Hitchcock, D.R.; Edwards, A.E. Streamflow and Nutrients from a Karst Watershed with a Downstream Embayment: Chapel Branch Creek. *J. Hydrol. Eng.* **2014**, *19*, 428–438. [CrossRef]
28. McCormack, T.; Naughton, O.; Johnston, P.M.; Gill, L.W. Quantifying the influence of surfacewater-groundwater interaction on nutrient flux in a lowland karst catchment. *Hydrol. Earth Syst. Sci.* **2016**, *20*, 2119–2133. [CrossRef]
29. Yue, F.J.; Li, S.L.; Zhong, J.; Liu, J. Evaluation of factors driving seasonal nitrate variations in surface and underground systems of a Karst Catchment. *Vadose Zone J.* **2018**, *17*, 170071. [CrossRef]
30. Yue, F.J.; Waldron, S.; Li, S.L.; Wang, Z.J.; Oliver, D.M. Land use interacts with changes in catchment hydrology to generate chronic nitrate pollution in karst waters and strong seasonality in excess nitrate export. *Sci. Total Environ.* **2019**, *696*, 134062. [CrossRef]
31. Cai, D.S.; Ma, Z.L.; Zhao, X.G.; Wang, K. Remote Sensing Supervision on Spatio-temporal Evolution of Karst Wetland in Recent 40 years in Huixian District of Guilin, China. *J. Guangxi Norm. Univ. Nat. Sci.* **2009**, *26*, 110–112. (In Chinese)
32. Peng, C.; Pan, X.D.; Jiao, Y.J.; Ren, K.; Zeng, J. Identification of Nitrate Pollution Sources Through Various Isotopic Methods: A Case Study of the Huixian Wetland. *Environ. Sci.* **2018**, *39*, 5410–5417. (In Chinese)
33. Li, L.X.; Li, J.C.; Wei, C.M.; Zhou, J.; Zhang, Q.; Liu, H.L. Analysis and evaluation of water quality status in Huixian wetland of Guangxi. *J. Guilin Univ. Technol.* **2019**, *39*, 693–699. (In Chinese)
34. Xing, M.L.; Li, H.X.; Jiang, L.; Tu, Y.; Zeng, H.F.; Wang, D.Q. Spatio-temporal characteristics of water pollutants in surrounding water system of Lingui and Huixian karst wetlands. *J. Guilin Univ. Technol.* **2019**, *39*, 168–176. (In Chinese)
35. Loucks, D.P.; Beek, E.V.; Stedinger, J.R.; Dijkman, J.P.M.; Villars, M.T. *Water Resources Systems Planning and Management: An Introduction to Methods, Models and Applications*; UNESCO: Paris, France, 2005.
36. Van Esbroeck, C.J.; Macrae, M.L.; Brunke, R.I.; McKague, K. Annual and seasonal phosphorus export in surface runoff and tile drainage from agricultural fields with cold temperate climates. *J. Great Lakes Res.* **2016**, *42*, 1271–1280. [CrossRef]
37. Soil Survey Staff. *Keys to Soil Taxonomy*, 12th ed.; USDA-Natural Resources Conservation Service: Washington, DC, USA, 2014.
38. National Environmental Protection Bureau (NEPB). *Standard Methods for the Examination of Water and Wastewater (Version 4)*; China Environmental Science Press: Beijing, China, 2002. (In Chinese)
39. National Environmental Protection Bureau (NEPB). *Water Quality—Determination of Total Nitrogen–Alkaline Potassium Persulfate Digestion UV Spectrophotometric Method (HJ636-2012)*; China Environmental Science Press: Beijing, China, 2012. (In Chinese)
40. National Environmental Protection Bureau (NEPB). *Water Quality—Determination of Nitrate-Nitrogen–Ultraviolet Spectrophotometric Method (HJ/T 346-2007)*; China Environmental Science Press: Beijing, China, 2007. (In Chinese)

41. National Environmental Protection Bureau (NEPB). *Water Quality—Determination of Ammonia Nitrogen–Nessler's Reagent Spectrophotometric Method (HJ535-2009)*; China Environmental Science Press: Beijing, China, 2009. (In Chinese)
42. National Environmental Protection Bureau (NEPB). *Water Quality—Determination of Phosphorus–Ammonium Molybdate Spectrophotometric Method (GB11893-89)*; China Environmental Science Press: Beijing, China, 1989. (In Chinese)
43. Ministry of Environmental Protection of China. *The Chinese Environmental Quality Standards for Surface Water (GB3838–2002)*; Ministry of Environmental Protection of China: Beijing, China, 2002. (In Chinese)
44. Bruun, J.; Pugliese, L.; Hoffmann, C.C.; Kjaergaard, C. Solute transport and nitrate removal in full-scale subsurface flow constructed wetlands of various designs treating agricultural drainage water. *Ecol. Eng.* **2016**, *97*, 88–97. [CrossRef]
45. Trang, N.T.T.; Shrestha, S.; Shrestha, M.; Datta, A.; Kawasaki, A. Evaluating the impacts of climate and land-use change on the hydrology and nutrient yield in a transboundary river basin: A case study in the 3S River Basin (Sekong, Sesan, and Srepok). *Sci. Total Environ.* **2017**, *15*, 586–598. [CrossRef] [PubMed]
46. Li, L.J.; Zhang, Q. Application of a surface runoff and groundwater coupled model to Xitiaoxi catchment. *J. Soil Water Conserv.* **2008**, *22*, 56–61.
47. Ou, Y.; Wang, X.Y.; Geng, R.Z. The influences of different landscape characteristics on water quality in the upper watershed of Miyun Reservoir. *Acta Sci. Circumst.* **2012**, *32*, 1219–1226.
48. Petry, J.; Soulsby, C.; Malcolm, I.; Youngson, A. Hydrological controls on nutrient concentrations and fluxes in agricultural catchments. *Sci. Total Environ.* **2002**, *294*, 95–110. [CrossRef]
49. Xu, B.; Shao, D.; Chen, S.; Li, H.; Fang, L. Response of water and nitrogen losses to water management practices and green manure application in lowland paddy fields. *J. Irrig. Drain. Eng.* **2017**, *143*, 05017007. [CrossRef]
50. Zhang, R.B.; Yao, Q.; Wang, P. A study on law of non-point source pollutants losses in a typical small watershed of Taihu basin—A case study at Meilin watershed in Yixing city of Jiangsu province. *Resour. Environ. Yangtze Basin* **2005**, *14*, 94–98. (In Chinese)
51. Xu, Q.G.; Liu, H.L.; Shen, Z.Y.; Xi, B.D. Characteristics on nitrogen and phosphorus losses in the typical small watershed of the Three Georges Reservoir area. *Acta Sci. Circumst.* **2007**, *27*, 326–331. (In Chinese)
52. Allan, J.D. Landscapes and Riverscapes: The Influence of Land Use on Stream Ecosystems. *Annu. Rev. Ecol. Evol. Syst.* **2004**, *35*, 257–284. [CrossRef]
53. Kim, J.; Choi, J.; Choi, C.; Park, S. Impacts of changes in climate and land use/land cover under IPCC RCP scenarios on streamflow in the Hoeya River Basin Korea. *Sci. Total Environ.* **2013**, *452–453*, 181–195. [CrossRef] [PubMed]
54. Minaudo, C.; Dupas, R.; Gascuel-Odoux, C.; Roubeix, V.; Danis, P.A.; Moatar, F. Seasonal and event-based concentration-discharge relationships to identify catchment controls on nutrient export regimes. *Adv. Water Resour.* **2019**, *131*, 103379. [CrossRef]
55. Evans, D.M.; Schoenholtz, S.H.; Wigington, P.J.; Griffith, S.M.; Floyd, W.C. Spatial and temporal patterns of dissolved nitrogen and phosphorus in surface waters of a multi-land use basin. *Environ. Monit. Assess.* **2014**, *186*, 873–887. [CrossRef] [PubMed]
56. Wiens, J.A. Spatial scaling in ecology. *Funct. Ecol.* **1989**, *3*, 385–397. [CrossRef]
57. Sliva, L.; Williams, D.D. Buffer zone versus whole catchment approaches to studying land use impact on river water quality. *Water Res.* **2001**, *35*, 3462–3472. [CrossRef]
58. Mostofa, A.M.G.; Karsten, H.D.; Veith, T.L.; Beegle, D.B.; Kleinman, P.J. Conservation dairy farming impact on water quality in a karst watershed in northeastern US. *Agric. Syst.* **2018**, *165*, 187–196.
59. Fan, R.H. Study on Nutrient Element Loss Process in a Small Watershed of Qianxi Rocky Desertification area. Master's Thesis, Guizhou University, Guiyang, China, June 2017. (In Chinese)
60. Uuemaa, E.; Palliser, C.C.; Hughes, A.O.; Tanner, C.C. Effectiveness of a Natural Headwater Wetland for Reducing Agricultural Nitrogen Loads. *Water* **2018**, *10*, 287. [CrossRef]
61. Wilcock, R.J.; Nagels, J.W.; Rodda, H.J.E.; O'Connor, M.B.; Thorrold, B.S.; Barnett, J.W. Water quality of a lowland stream in a New Zealand dairy farming catchment. *N. Z. J. Mar. Freshw. Res.* **1999**, *33*, 683–696. [CrossRef]
62. Yang, T. Analysis of the Removal Efficiency of Total Nitrogen and Total Phosphorus through Luoshijiang Wetland. *J. Environ. Sci.* **2015**, *2*, 45–47. (In Chinese)

63. Pan, L.Y.; Dai, J.F.; Yu, C.W.J.; Xie, X.L.; Wu, Z.Q. Spatial-temporal Features of Nitrogen and Phosphorus Losses of Jingui River Watershed in the upstream of Lijiang River. *IOP Conf. Ser. Earth Environ. Sci.* **2019**, *304*, 022073. [CrossRef]
64. Lin, P. The Characteristics of Non-point Source Pollution and Control Technology Demonstration Research on Li River Watershed. Master's Thesis, Guilin University of Technology, Guilin, China, June 2016. (In Chinese)
65. Sickman, J.O.; Leydecker, A.; Chang, C.C.Y.; Kendall, C.; Melack, J.M.; Lucero, D.M.; Schmiel, J. Mechanisms underlying export of N from high- elevation catchments during seasonal transitions. *Biogeochemistry* **2003**, *64*, 1–24. [CrossRef]
66. Burns, D. What do hydrologists mean when they use the term flushing? Invited commentary. *Hydrol. Process.* **2005**, *19*, 1325–1327. [CrossRef]